Journal of Analytical Science and Technology

RESEARCH ARTICLE Open Access

MgO-ZnO/carbon nanofiber nanocomposite as an adsorbent for ultrasound-assisted dispersive solid-phase microextraction of carbamazepine from wastewater prior to high-performance liquid chromatographic detection

Malesela William Lekota[1], K. Mogolodi Dimpe[1] and Philiswa Nosizo Nomngongo[1,2,3*]

Abstract

A simple, rapid, and efficient ultrasound-assisted dispersive solid-phase microextraction (UA-DSPME) method was developed for the preconcentration of carbamazepine (CBZ) in wastewater prior to high-performance liquid chromatography coupled with diode array (HPLC-DAD) determination. The carbon nanofibers coated with magnesium oxide-zinc oxide (MgO-ZnO@CNFs) nanocomposite was used as an efficient adsorbent in magnetic dispersive solid-phase microextraction method. The structural and morphological properties of the nanocomposite were characterized by scanning electron microscopy and energy dispersive spectroscopy, transmission electron microscopy, X-ray diffractometer, and Fourier transform infrared spectroscopy. The surface area was investigated using Brunauer–Emmett–Teller. Several factors (such as pH, mass of adsorbent, extraction time, and eluent volume) that affect extraction and preconcentration of CBZ were also assessed and optimized using response surface methodology based on central composite design. Under optimal conditions, the limits of detection (LOD) and quantification were 0.08 μg L^{-1} and 0.29 μg L^{-1}, respectively. The calibration curve constructed after preconcentration of seven successive standards was linear in the concentration range of 0.3–800 μg L^{-1} with the correlation coefficient of 0.9922. The intra-day and inter-day precisions expressed in terms of relative standard deviation were 1.4% and 4.2%. A preconcentration factor of 490 was achieved, and the method was applied for the analysis of spiked wastewater. Satisfactory recoveries ranging from 97.8 to 102% were obtained.

Keywords: MgO-ZnO@CNFs nanocomposite, Dispersive solid-phase microextraction, Carbamazepine, Desirability function

Introduction

In the last decades, there have been more reports of pharmaceutical compounds that are present in rivers and surface waters at large (Andreozzi et al. 2002). The ever-increasing demand of medicine for treatment of various diseases and disorders in veterinaries and humans has been recognized as the major source of these compounds that are polluting our waters (Halling-Sørensen et al. 1998). When these pharmaceuticals are consumed, they are metabolized by the body and excreted out through defecation and urination as glucuronides and sulfates. However, some of them remain intact and are not converted to other compounds (Ternes 1998). Besides the substances that remain metabolized, numerous other substances are transformed into active metabolites (Hoff et al. 2015). Defecation and urination are not the only sources of this type of environmental pollution but inappropriate disposal of unused and

* Correspondence: pnnomngongo@uj.ac.za
[1]Department of Chemical Sciences (Former Applied Chemistry), University of Johannesburg, Doornfontein Campus, P.O. Box 17011, Doornfontein 2028, South Africa
[2]DST/Mintek Nanotechnology Innovation Centre, University of Johannesburg, Doornfontein 2028, South Africa
Full list of author information is available at the end of the article

expired medicine also contribute to pollution (Murdoch 2015). Some of these pharmaceutical compounds or their metabolites are very stable and mobile in natural environmental conditions (Murdoch 2015). Since the water treatment plants fail to remove them, they can be deposited into the soil which may reach the agricultural land (Larsen et al. 2004). Compounds that reach the surface water are likely to contaminate sources that are used for drinking water (Miao et al. 2005). Through intensive studies all over the world in the last few decades, some pharmaceutical compounds have been successfully detected in groundwater (Heberer 2002a; Heberer 2002b; Sacher et al. 2001).

One of the widely used drugs for the treatment of disorders is carbamazepine (CBZ). Generally, CBZ is defined as a synthetic drug that falls under the benzodiazepine class and it is primarily used for treating epileptic disorders (Gierbolini et al. 2016). This drug does not only help epileptic patients control seizures but it is also used for the treatment of bipolar, nerve disorders, and psychiatric therapy, and it can also be used in trigeminal neuralgia treatment (Chen and Lin 2012). This drug is primarily digested by bile which is a fluid released from the liver where it is partially metabolized into CBZ 10, 11 epoxides, and other derivatives (Swart et al. 1998). Similar other pharmaceutical drugs, its main sources are defecation, urination, and improper disposal of expired or unused. When an average person takes CBZ, about 2 to 3% of it remains as a parent compound and it is released through urination and flushed down where it is mixed with wastewater (Clara et al. 2004). Studies that were conducted in Europe and North America have indicated that this drug has been detected most frequently in wastewater treatment plants, effluents, and river streams (Heberer 2002a; Metcalfe et al. 2003; Öllers et al. 2001; Ternes 1998). CBZ has been found in high concentrations, up to several ng L^{-1} in surface waters (Clara et al. 2004; Ternes 1998). In Germany, this drug has been detected at a concentration of 1075 ng L^{-1} in the surface waters of the city of Berlin (Heberer 2002a).

The development of quick, accurate, affordable, easy to use, and sensitive methods for detection, preconcentration, and removal of CBZ at trace levels is necessary and has been one of the greatest challenges faced by an analytical chemist for years. Recent analytical methods are based mostly on the use of liquid chromatography-tandem mass spectrometry (LC–MS/MS) (Lübbert et al. 2017). This is because this technique is highly sensitive and can detect and identify compounds at extremely low concentrations, but it is very complicated and expensive so not all the labs can afford it (Gros et al. 2006). Therefore, several sample preparation methods have been developed to increase the detection limits of analytical detection techniques such as HPLC coupled with a UV detector (Vosough et al. 2014) and gas chromatography-flame ionization detector (Bahmaei et al. 2018). These methods include solid-phase microextraction (SPME) (Asgari et al. 2017), solid-phase extraction (SPE) (dos Santos et al. 2017; Fortuna et al. 2010; Mirjana et al. 2012; Patrolecco et al. 2013), ultrasound-assisted emulsification microextraction (UAEME) (Bahmaei et al. 2018), dispersive liquid–liquid microextraction (DLLME) (Behbahani et al. 2013), and solid-phase extraction combined with dispersive liquid–liquid microextraction (Rezaee and Mashayekhi 2012). Among the abovementioned sample preparation techniques, dispersive solid-phase microextraction (DSPME) has attached significant attention due to attractive properties such as rapidity, less solvent consumption, simplicity, and economical (Asfaram et al. 2015a; Asfaram et al. 2015b). Similar to traditional SPE, the nature of adsorbent plays a fundamental role in the extraction and preconcentration process (Asfaram et al. 2015a; Asfaram et al. 2015b).

Recently, nanostructured adsorbents have received significant attention because of their attractive properties such as high adsorption capacity, chemical and thermal stability, and high surface area (Zhang et al. 2011). Among other nanomaterials, carbon-based adsorbent nanomaterials display superior mechanical, chemical, and physical properties (Asmaly et al. 2015). Carbon nanofibers (CNFs) are carbon-based adsorbent nanomaterials that are classified as sp^2-based linear filaments that have a very large surface area. The structure of carbon nanofibers is what gives it its exceptional properties and unlimited applicability (Kaerkitcha et al. 2016). These properties allow CNT to have good potential for organic pollutant removal from water. In addition, carbon nanofibers have a large surface area, developed porosity, and tunable surface-containing functional groups which enhance their adsorption efficiency (Asmaly et al. 2015). However, the main challenge of CNFs as adsorbent is separating them from aqueous solutions (Chaba and Nomngongo 2018). This limitation can be overcome by incorporating metal-based nanomaterials. In this work, the excellent adsorption properties of CNFs, the molecular sieve effects of ZnO nanoparticles, and high adsorption capacity of MgO were combined to form ZnO-MgO@CNF nanocomposite. The attractive feature of ZnO-MgO@CNF nanocomposite lies in the characteristics of CNFs as they are able to bond with various metal oxides without their own extraction properties being jeopardized and instead become enhanced (Karimi et al. 2015). Due to their high surface area per volume, they can accommodate the metal oxide particles in larger numbers and their unique morphologies enhance the adsorption capacity (Kaerkitcha et al. 2016).

Therefore, in this work, a much cheaper, fast, and simpler method utilizing a preconcentration procedure based on ultrasound dispersive solid-phase microextraction (DSPME) for analysis CBZ in wastewater is used.

The analyte was quantified using high-performance liquid chromatography coupled with diode array as a detector (HPLC-DAD). The success of the UA-DSPME method was by use ZnO-MgO@CNF nanocomposite as an adsorbent. The influential experimental variables such as the sample pH, eluent volume, mass of adsorbent, and extraction time were investigated and optimized using the response surface methodology based on central composite design and desirability function.

Methods

Material and reagents

All chemicals were of analytical reagent grade unless otherwise stated, and ultra-pure water (Direct-Q® 3UV-R purifier system, Millipore, Merck) was used throughout the study. Carbamazepine, carbon nanofibers, sodium hydroxide methanol, $Mg(NO_3)_2 \bullet 6H_2O$, ethanol, $Zn(AC)_2$, and acetonitrile (HPLC, ≥ 99%) were purchased from Sigma-Aldrich (St. Louis, MO, USA). Stock solutions of carbamazepine (10 mg/mL) were prepared in ultra-pure water. Working standards of 1000 ng/mL were prepared daily by diluting appropriate volumes of the stock solution in ultra-pure water.

A 100 mg L^{-1} stock solution of CBZ was prepared by dissolving appropriate amounts in small amounts of methanol, diluted with ultra-pure water and stored at 4 °C. Working solutions (1 mg L^{-1}) was used to prepare calibration standards ranging from 50–6000 ng mL^{-1}.

Instrumentation

An OHAUS starter 2100 pH meter (Pine Brook, NJ, USA) was used for pH adjustments of the reagents and to measure the pH of samples. The dispersion was carried out using an ultrasound bath (Bandelin Sonorex Digitec, Bandelin electronic GmbH & Co. KG, Berlin, Germany). All the reactions were stirred using a Labcon 3075U hotplate and magnetic stirrer (Labdesign Engineering, Maraisburg, RSA), and all the drying was done using an oven (EcoTherm, Labotec, Midrand, Johannesburg, South Africa). The scanning electron microscopy coupled with energy-dispersive X-ray spectroscopy (SEM/EDS TESCAN VEGA 3 XMU, LMH instrument (Czech Republic)) was used for morphological and elemental characterization. The nanostructure and particle size of the adsorbent were studied using transmission electron microscopy (TEM, JEM-2100, JEOL, Tokyo, Japan). The functional groups and structural properties of the adsorbent were determined using PerkinElmer spectrum 100 Fourier transform infrared spectrometer (Waltham, MA, USA). The XRD measurements were carried out using PANalyticalX'Pert X-ray Diffractometer (PANalytical BV, Netherlands) using a Cu Kα radiation (λ = 0.15406 nm) in the 2θ range 4–90 at room temperature.

Synthesis of ZnO-MgO@CNF nanocomposite

The synthesis of the nanocomposite was carried out according to previous studies with some modification (Aslani et al. 2011). To describe the method briefly, a 10-mmol solution of $Zn(AC)_2$ was dissolved in 50 mL of methanol and added to a 10-mmol solution of $Mg(NO_3)_2 \bullet 6H_2O$ that was also dissolved in 50 mL of methanol. Then, 4 g of CNFs was added to the mixture. The mixture was then sonicated for 15 min to disperse the CNFs in the solution. Ten milliliters of sodium hydroxide solution (10 mol L^{-1}) was then added to the above mixture at room temperature under magnetic stirring. After 30 min of stirring, the mixture was transferred into Teflon-lined stainless steel autoclaves, sealed, and maintained at 160 °C for 12 h. Subsequently, the reactor was cooled down to room temperature. The resulting solid products were centrifuged and subsequently washed with distilled water and methanol to remove the ions possibly remaining in the final products. The resultant product was dried at 60 °C in an oven for 12 h followed by calcination at 500 °C for 2 h to ensure proper formation of ZnO and MgO.

Chromatographic conditions

An Agilent 1200 Infinity series HPLC equipped with a diode array detector (Agilent Technologies, Waldbronn, Germany) was used to perform the analyses. The mobile phase consisting of acetonitrile and ultra-pure water in the ratio of 30:70 (*v*/*v*) was pumped through the column (C18) at the flow rate of 1.0 mL min^{-1} with an injection volume of 10 μL. The column oven compartment was maintained at 25 °C, and the detection was carried out at a wavelength of 220 nm. Fresh working samples were prepared for each day, and new calibration was constructed. The solutions were filtered through a phenomenex membrane of 0.45 mm pore size (25 mm filter) and transferred to an auto-sampler vial for further analysis. Calibration curves were constructed using peak area versus concentration of the standard solutions. The typical chromatograms for the standard solution are shown in Fig. 1 and the retention time of 9.2 min.

Sampling and sample collection

Influent (after sediment removal) and effluent wastewater samples were collected from Daspoort (Pretoria, Gauteng, South Africa) wastewater treatment plant. All the samples were collected in precleaned 500 mL glass bottles. The samples were then refrigerated at 4 °C. The physicochemical parameters such as chemical oxygen demand (COD), pH, turbidity, total dissolved solid (TDS), total organic carbon (TOC), and conductivity were investigated. The physicochemical measurements for characterization of wastewater samples are presented in Table 1.

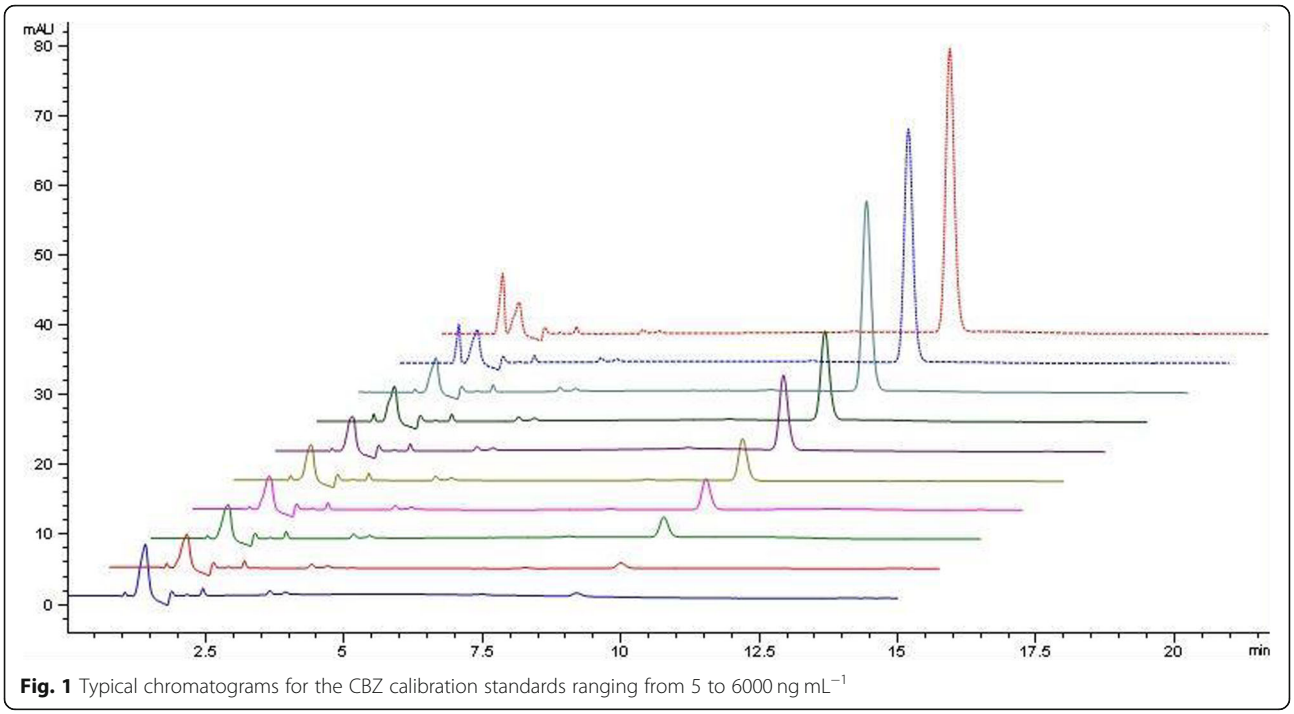

Fig. 1 Typical chromatograms for the CBZ calibration standards ranging from 5 to 6000 ng mL^{-1}

Ultrasound-assisted dispersive solid-phase microextraction procedure

The extraction and preconcentration procedure based on UA-DSPME was carried according to the previous studies (Nyaba et al. 2016). About 20–60 mg of ZnO-MgO@CNF nanocomposite was first rinsed with 5 mL methanol followed 5 mL of ultra-pure water. The adsorbent was then dispersed by ultrasonication into 10 mL aqueous sample solution containing 100 ng L^{-1} of CBZ (sample pH 4–9) for 5–30 min to form a homogeneous suspension. The adsorbent and supernatant were separated through centrifugation at 3600 rpm for 5 min and the liquid was decanted. About 500–1000 μL of acetonitrile (eluent) was added into the residual adsorbent. The desorption of the analyte from the adsorbent was achieved by ultrasonication for 5 min. Finally, the eluent containing the analyte (supernatant) and the adsorbent were separated by centrifugation for 5 min. The supernatant was filtered into a HPLC vial followed by HPLC for analysis. A flow diagram summarizing the extraction and preconcentration processes is presented in Fig. 2.

Table 1 Physical-chemical parameters of influent and effluent samples

Parameters	Influent	Effluent
pH	7.61	7.11
TDS (mg/L)	328	198
COD (mg O_2/L)	177	17.5
BOD_5 (mg O_2/L)	123	0.15
Conductivity (μS/cm)	678	208
TOC (mg/L)	115	19.3

Results and discussion

Characterization

X-ray diffraction (XRD)

Figure 3 shows the XRD patterns of (a) CNFs, (b) ZnO, (c) MgO-ZnO@CNF nanocomposite, and (d) MgO (their characteristic peaks shown in Additional file 1). The XRD pattern in Fig. 3 a shows the CNF spectrum with a characteristic peak at 25.9° which was assigned to the (002) plane of a CNF graphite structure. However, this peak cannot be observed in Fig. 3 c which is the nanocomposite because of high crystallinity and reduced composition of CNFs. Figure 3 b represents the XRD pattern of ZnO which is in full agreement with JCPDS 36-1451 (Dinesh et al. 2014), and the crystals correspond to the hexagonal system with unit cell length as 3.2539 Å. The crystallite sizes of the ZnO, MgO, and CNF products were determined by using Debye Scherrer's formula:

$$D = \frac{k\,\lambda}{\beta\,\mathrm{Cos}\theta}$$

where, $k = 0.9$ is the shape factor, λ is the X-ray wavelength of CuKα1 radiation, β is the full width at half maximum (FWHM) of the peaks, and θ is the glancing angle.

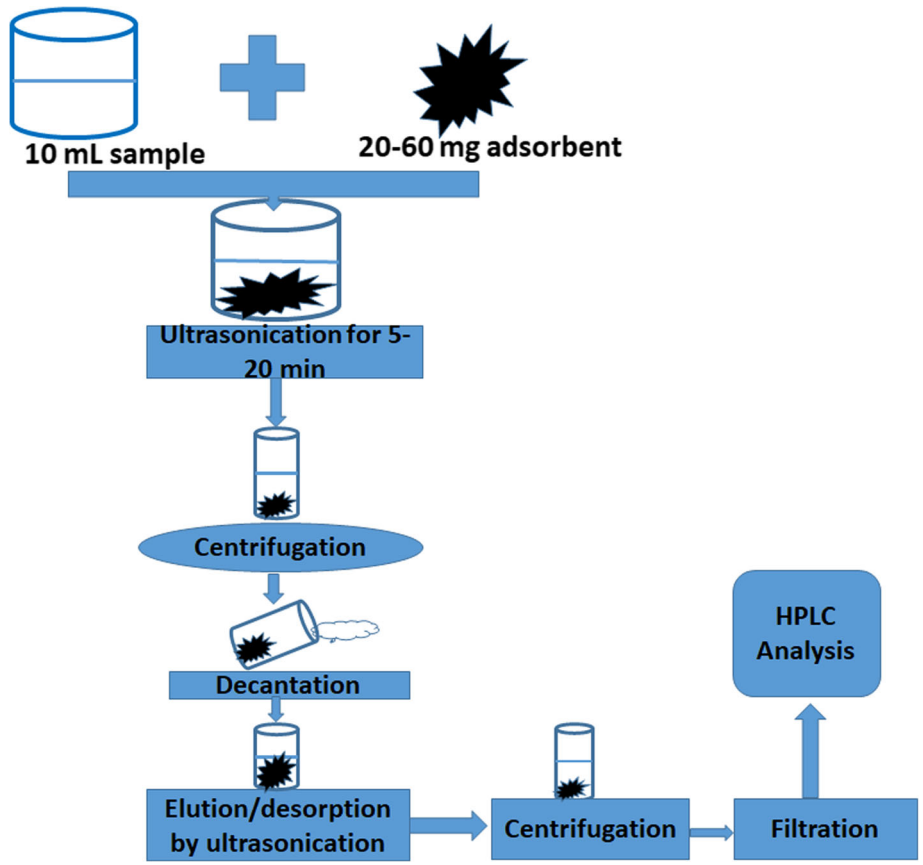

Fig. 2 Flow diagram showing the extraction and preconcentration steps

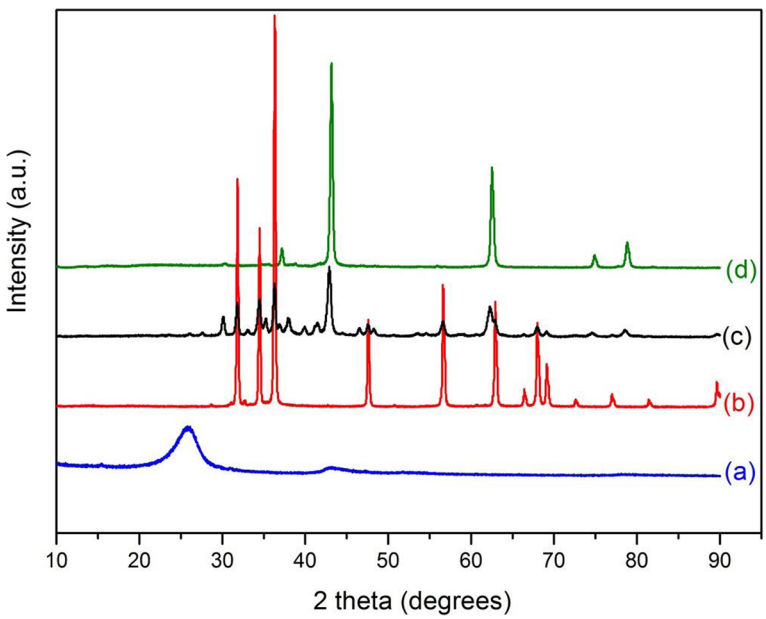

Fig. 3 XRD pattern of **a** CNFs, **b** ZnO, **c** MgO-ZnO@CNFs, and **d** MgO

The average crystallite sizes were found to be 36.3 nm (ZnO), 26.9 nm (MgO), and 12.3 nm (CNFs). Figure 3 d shows the oxide as magnesium oxide and magnesium hydroxide ($Mg(OH)_2$). The peaks at 37.3° (111) and 74.9° (311) were assigned to $Mg(OH)_2$. This XRD is in total agreement with JCPDS 89-7746 (Dhineshbabu et al. 2014), and the crystals correspond to the cubic system with unit cell length as 4.21 Å. The broad peaks resonating at (200), (220), and (222) diffraction planes show the ultra-fine nature and the tiny crystallite sizes and reveal the cubic phase of MgO nanoparticles. Figure 3 c represents the MgO-ZnO@CNF nanocomposites, and all the peaks visible in Fig. 3 a, b, and d are seen in this figure. This indicates the successful incorporation of MgO and ZnO on to the surface of CNFs.

Scanning electron microscopy (SEM) and energy-dispersive spectroscopy (EDS)

The morphology of the carbon nanofibers is shown in Fig. 4 a, and the SEM image illustrated that the CNFs are typically cylindrical in shape but also consist of bamboo-shaped nanofibers. The SEM images also suggest that the length of the CNFs is up to several micrometers. Figure 4 b illustrates the porous structures of MgO-ZnO nanocomposite that is also visible in Fig. 4 c which represent the MgO-ZnO@CNF nanocomposite. It can be seen from Fig. 3 c that the ZnO-MgO nanoparticles were scattered onto the surface CNFs. This is also supported by EDS in Fig. 4 d which shows the elemental composition present, and their relative weight percentages were 33.5%, 29.5%, 18%, and 15.6% O, Mg, C, and Zn, respectively. These results further confirm the incorporation of ZnO-MgO on the surface of the CNFs.

Transmission electron microscopy (TEM)

The typical cylindrical and bamboo-shaped carbon nanofibers as illustrated in Fig. 5 a. The TEM results are consistent with the SEM results, and it can be observed that the cylindrical hollow fibers have smooth outer walls that are

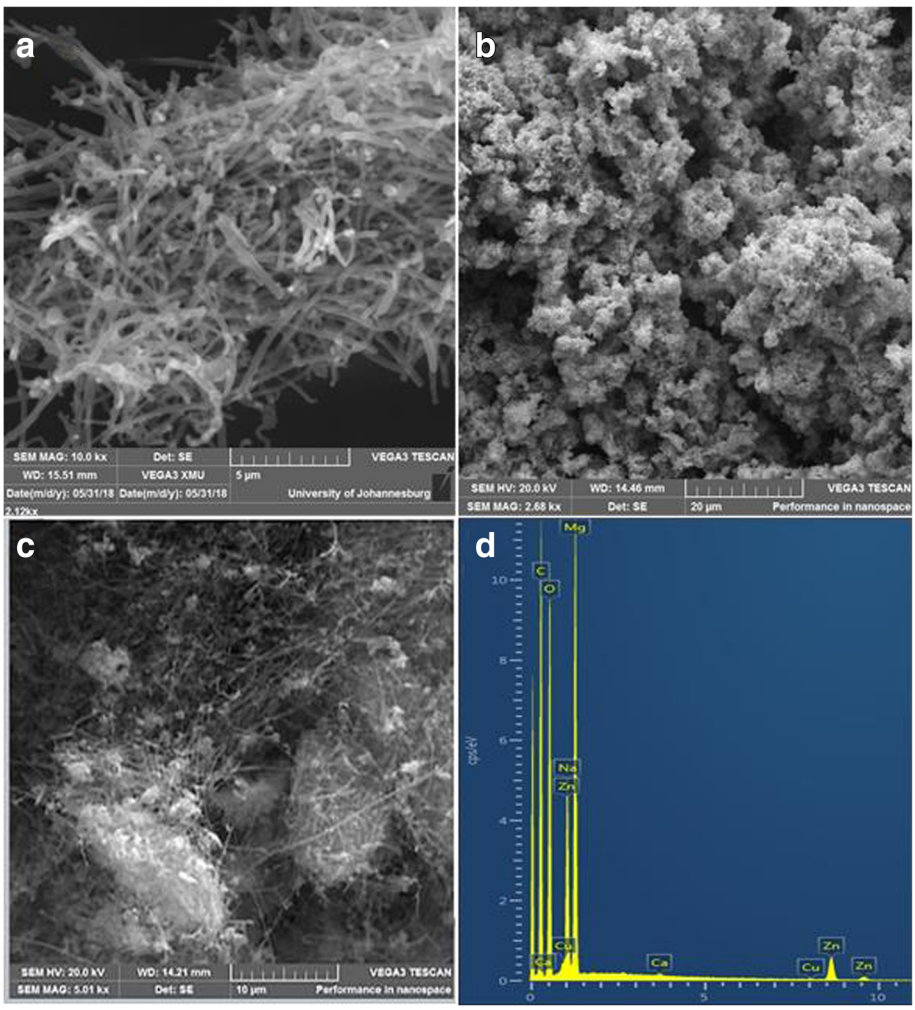

Fig. 4 SEM images of **a** CNFs, **b** MgO-ZnO, **c** MgO-ZnO@CNFs, and **d** EDX of MgO-ZnO@CNFs nanocomposite

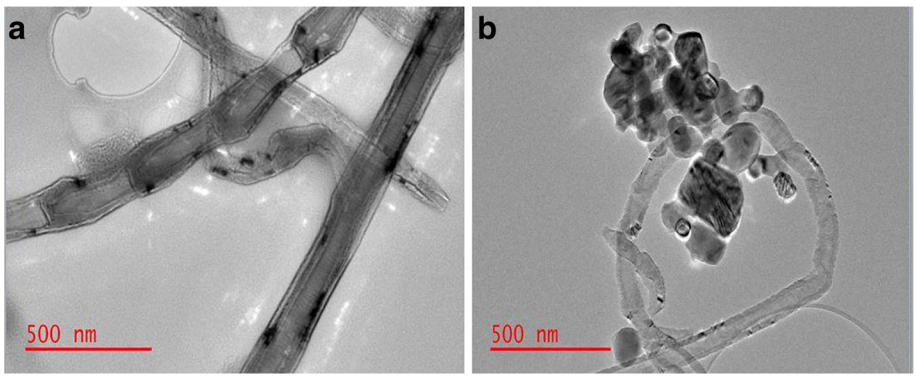

Fig. 5 TEM images of **a** CNFs and **b** ZnO-MgO@CNFs taken at 500 nm

uniform and made of distinct sandwich of graphite layers. These graphite layers are parallel with respect to the axes of the fibers and display and almost defect-free material. The bamboo-shaped fibers on the other hand display some areas of defects and change in diameter in different areas. This is because these types of fibers are composed of multi-walled graphite structures (Kaerkitcha et al. 2016). Figure 5 b shows how the ZnO-MgO nanoparticles were dispersed onto the CNFs. This figure shows that the ZnO-MgO nanoparticles were significantly larger than the CNFs in diameter. The average particles size of the nanocomposite ranged from 56.3–108 nm. This is also in agreement with BET results that show a significant increase in surface area.

Brunauer–Emmett–Teller (BET)

The BET surface area of CNFs was found to be 21.1 $m^2 g^{-1}$ and that of MgO-ZnO@CNFs was found to be 121 $m^2 g^{-1}$, which means that the incorporation of MgO-ZnO brought more than 500% increase the surface area of CNFs, therefore providing more adsorption sites for the analyte. The pore volume of CNFs was found to be 0.12 $cm^3 g^{-1}$ and that of the MgO-ZnO@CNFs nanocomposite was found to be 0.65 $cm^3 g^{-1}$ which is also a significant increase that allows more particles of the analyte to be adsorbed on the pores of the composite. The adsorption average pore diameter of the nanocomposite was found to be 21.6 nm.

Fourier transform infrared spectroscopy (FTIR)

Fourier Transform infrared spectroscopy was used to investigate the structural propertied of the nanocomposite. The bands that at 483 and 524 cm^{-1} correspond to the absorption peaks of Zn–O bond and verify the presence of ZnO, the same peaks can be observed on Fig. 6 c. The characteristic peaks observed at 508 and 410 cm^{-1} correspond to the Mg–O bending vibrations present in both Fig. 6 c and d. This confirms the presence of MgO in the nanocomposite. The band at 3132, 3426, 3445, and 3428 cm^{-1} arises from the stretching and bending of the O–H group present in the moisture absorbed from the atmosphere. The peaks at 1775 and 1448 cm^{-1} arise from the stretching of C=C and C–C bonds, respectively, which corresponds to CNFs. These peaks can be observed in Fig. 5 d but with a slight shift to 1636 and 1410 cm^{-1}, respectively. This shift towards higher wavenumbers is due to the decrease in mass of CNFs in the nanocomposite.

Optimization of separation and preconcentration method

Two-level fractional factorial design

In order to achieve optimum conditions, a two-level fractional factorial design with 12 experiments was conducted to investigate the effect of eluent volume (EV), extraction time (ET) mass of adsorbent (MA), and pH on the recovery (%R) of CBZ after adsorption as presented in Table 2. The results in Table 2 were investigated statistically, and the analysis of variance (ANOVA) results was presented in the form of Pareto chart (Fig. 7). As seen, sample pH and the mass of adsorbent were significant at 95% confidence level. These findings suggested that the mass of adsorbent (MA) and sample pH require further optimization. Eluent volume was as added as the third parameter because it was observed in Table 2 that the increase of eluent volume increases the response. In addition, it was observed that improved recoveries were observed at experiments 9–12 (central points). This might be due to relatively high MA and EV as well as slightly higher pH. This experiment area is in agreement with the observation in Fig. 7 whereby pH values lower than 9 and higher masses will increase the response (%recovery). Therefore, the central composite design should be used for further optimization of the three factors.

Response surface methodology (RSM)

Response surface methodology (RSM) provides better knowledge regarding the interactions between individual variables. It also allows the achievement optimal conditions for each investigated variable that will lead to the attainment of the maximum analytical response (Asfaram et al. 2015a). The three-dimensional response

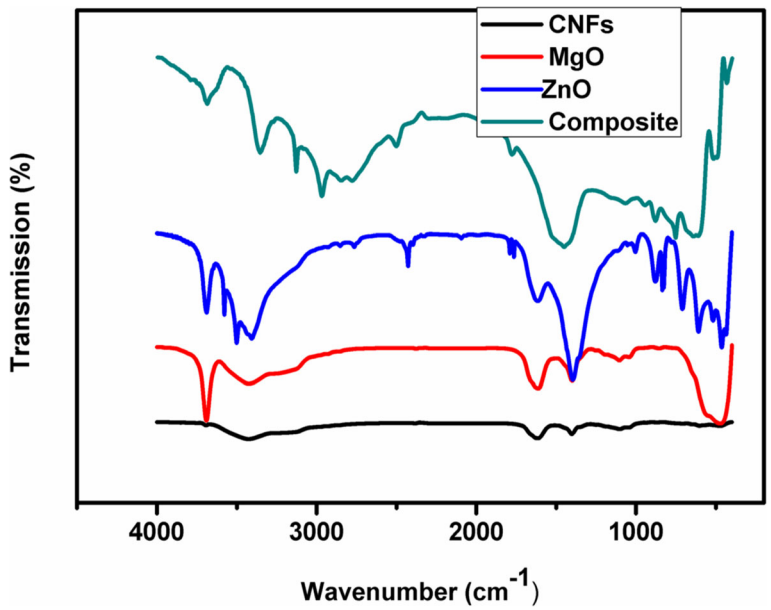

Fig. 6 FTIR spectrum of ZnO (blue), MgO (Red), MgO-ZnO@CNFs (green), and CNFs (black)

surfaces showing the combined effects of two factors on the analytical response at a constant and fixed level of other variables (central point) are presented in Fig. 8. As seen in Fig. 8 a and c, at MA values higher than 20 mg the %R increased and the maximum analytical response was obtained when sample pH was 6–7. Figure 8 b shows the desorption of the CBZ analytes from the surface of MgO-ZnO@CNF nanocomposite with respect to the pH increased with increasing pH and eluent volume. Figure 8 a and b indicate that at pH of between 6 and 7, about 100% of CBZ is adsorbed and recovered. The %R decreased as the pH is lower or higher than 6–7. This is due to the protonation and deprotonation of surface functional groups of CBZ as well as the MgO-ZnO@CNF nanocomposite.

Table 2 Optimization parameters and their corresponding values for dispersive solid-phase microextraction of CBZ. *C* central point or middle value

Experiment no.	EV/uL	MA/mg	ET/min	pH	%R
1	500	20	5	4	22.2
2	1000	20	5	9	42.5
3	500	60	5	9	48.5
4	1000	60	5	4	57.9
5	500	20	30	9	29.2
6	1000	20	30	4	24.9
7	500	60	30	4	40.5
8	1000	60	30	9	86.2
9 (C)	750	40.	17.5	6.5	95.7
10 (C)	750	40	17.5	6.5	95.4
11 (C)	750	40	17.5	6.5	95.1
12 (C)	750	40	17.5	6.5	95.8

The optimization of the investigated parameters was further investigated using the desirability function (Fig. 9) . The lines observed in Fig. 9 demonstrate the ranges of parameters with the exact values of each factor, and this information was obtained from the RSM model (Asfaram et al. 2015b). The variation of %R with respect to the RSM model variables is described by the bottom lines while the vertical lines demonstrate that sample pH, the mass of adsorbent, and eluent volume were optimum at 6.5, 74 mg, and 1170 μL, respectively. These conditions led to a maximum of 102% with the desirability of 1.00. The model was validated experimentally, and the experimental value ($N = 6$) and the predicted value of CBZ recovery were 99.7 ± 1.1% and 102%, respectively, suggesting the validity and applicability of the RSM model.

Analytical performance of the UA-DSPE/HPLC-DAD method

Under optimum conditions, the analytical performance of the proposed UA-DSPME/HPC-DAD method for preconcentration and determination of CBZ was evaluated. Several parameters such as the linear range, precision expressed as relative standard deviation (RSD), limit of detection (LOD), limits of quantification (LOQ), and preconcentration factor were assessed and the results are tabulated in Table 3. The LOD and LOQ were calculated as three or ten times the standard deviation ($n = 10$) of the lowest concentration of the calibration curve after preconcentration. The UA-DSPME/HPC-DAD method was

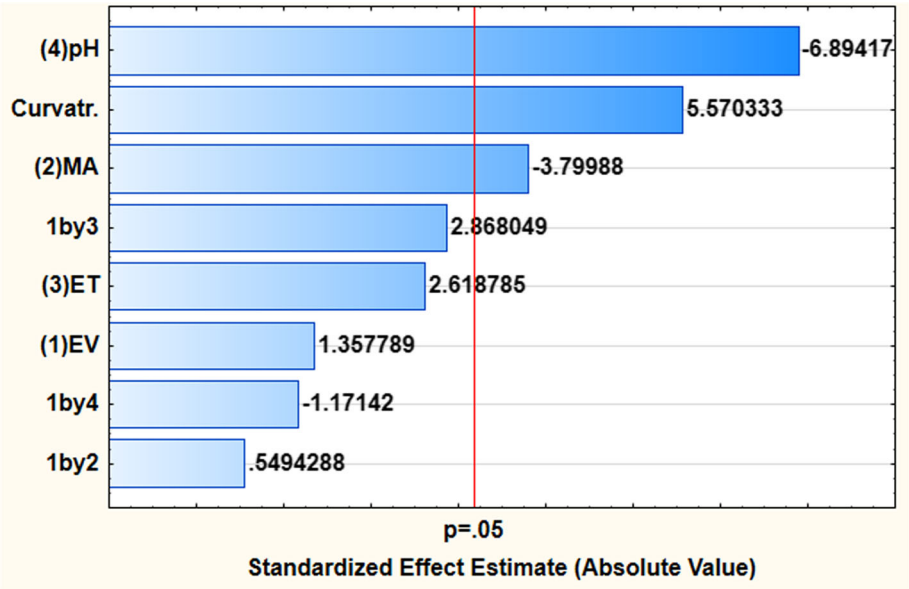

Fig. 7 Pareto chart of standardized effects for variables in the preconcentration of CBZ

found to have a linear dynamic range with a correlation coefficient of 0.9922. The repeatability was evaluated for ten independent measurements for 100 ng mL^{-1} CBZ concentration performed the same way in 1 day, and the reproducibility was for five working days. As seen, the relative standard deviations (%RSD) were less than 5% and this implied that the method had good precision. Finally, the preconcentration factor (PF) was calculated as the ratio of the slopes after and before preconcentration.

Validation and application

The accuracy of the UA-DSPME/HPLC-DAD procedure was evaluated using a wastewater sample spiked and unspiked from Daspoort (Pretoria, Gauteng, South Africa)

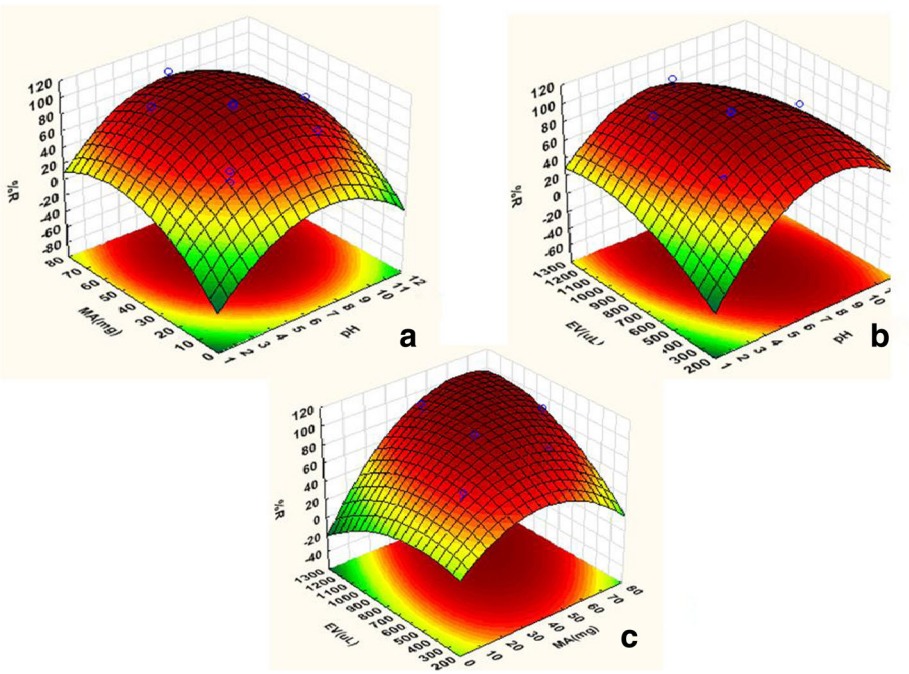

Fig. 8 Response surface and contour plots of the combined effects of **a** mass of adsorbent and pH, **b** eluent volume and pH, and **c** eluent volume and mass of adsorbent

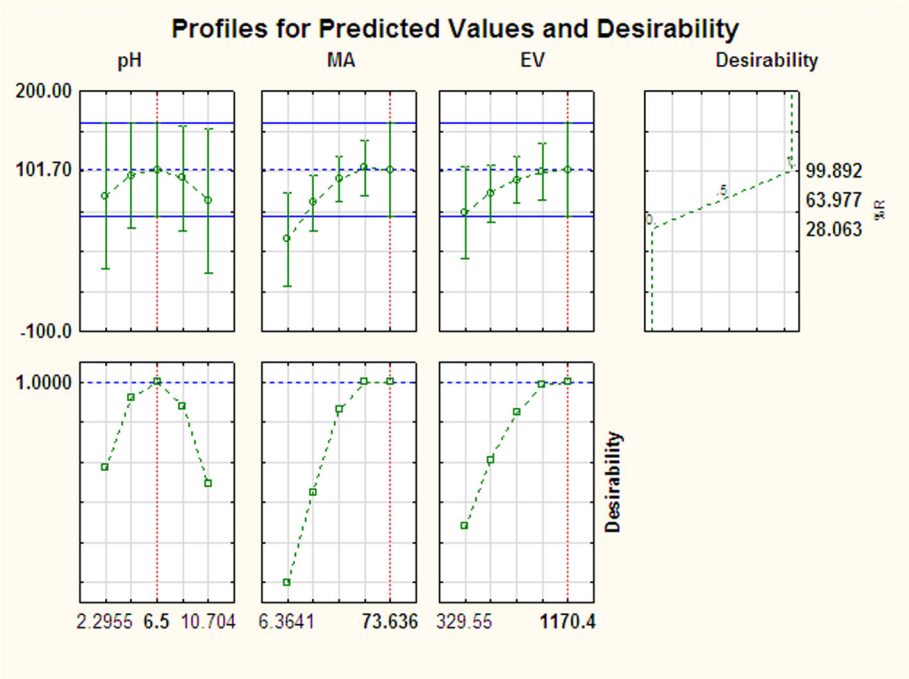

Fig. 9 Profiles for experimental and predicated values and desirability function for the recovery of CBZ

wastewater treatment plant. The water samples were spiked with two different concentrations as shown in Table 4. As seen, the recoveries were between 97.8% and 102% with %RSD less than 5%. These results suggested that CBZ can be quantitatively recovered from the real samples using the developed method. In addition, the results show the ability of UA-DSPME/HPLC-DAD method to extract, preconcentrate, and determine the amount of CBZ in real wastewater samples.

Conclusion

An efficient ultrasound-assisted dispersive solid-phase microextraction was developed as sample pretreatment method for extraction and preconcentration of carbamazepine in wastewater samples prior to analysis by HPLC-DAD. The optimum conditions for extraction and preconcentration of CBZ from wastewater samples were obtained using a response surface methodology based on central composite experimental design. The analytical results obtained demonstrated that the MgO-ZnO@CNF nanocomposite as an adsorbent was suitable for extraction CBZ. Attractive features of the method included low LOD, relatively short analysis, low consumption of sample and adsorbent, reasonably high preconcentration factor, wide linear dynamic range, and excellent recoveries with high accuracy and precision.

In addition, the ZnO-MgO@CNF nanocomposite displayed intriguing properties because it combined the best features of each component in the composite and can be a great turning point in water treatment as it can also be used for water purification.

Table 3 Analytical figures of merit of the applied UA-DSPME/HPLC-DAD method for preconcentration of CBZ

Analytical figures of merit	Values
Regression equation before preconcentration	$y = 0.073x + 6.7261$
Regression equation after preconcentration	$y = 35.735x + 12.972$
Linear range (ng mL^{-1})	0.1–800
Limit of detection (LOD) (ng mL^{-1})	0.08
Limit of quantification (LOQ) (ng mL^{-1})	0.29
Repeatability (RSD, %) ($N = 10$)	1.4
Reproducibility (RSD, %) ($N = 5$)	4.2
Preconcentration factor (PF)	490

Table 4 Recoveries of CBZ from wastewater samples spiked at two levels (100 ng mL^{-1} and 500 ng mL^{-1}) using the proposed UA-DSPME/HPLC-DAD method, $n = 3$

Sample	Added (ng mL^{-1})	Found (ng mL^{-1})	Recovery
Effluent 1	0	574 ± 8	–
	100	674	99.7
	500	1083 ± 15	102
Influent 1	0	836 ± 8	
	100	934 ± 12	97.8
	500	1430 ± 18	99.1

Additional file

Additional file 1: Table S1. Materials with their corresponding angles and phases. (DOC 30 kb)

Abbreviations

ANOVA: Analysis of variance; CBZ: Carbamazepine; COD: Chemical oxygen demand; DLLME: Dispersive liquid–liquid microextraction; EDS: Energy-dispersive spectroscopy; ET: Extraction time; EV: Eluent volume; HPLC-DAD: High-performance liquid chromatography coupled with diode array; LOD: Limits of detection; LOQ: Limits of quantification; MA: Mass of adsorbent; MgO-ZnO@CNFs: Carbon nanofibers coated with magnesium oxide-zinc oxide; PF: Preconcentration factor; RSD: Relative standard deviations; RSM: Response surface methodology; SEM: Scanning electron microscopy; SPE: Solid-phase extraction; SPME: Solid-phase microextraction; TDS: Total dissolved solid; TEM: Transmission electron microscopy; TOC: Total organic carbon; UA-DSPME: Ultrasound-assisted dispersive solid-phase micro-extraction; UAEME: Ultrasound-assisted emulsification microextraction; XRD: X-ray diffraction

Acknowledgements

The authors wish to thank the University of Johannesburg (UJ), Department of Applied Chemistry for providing their laboratory facilities.

Authors' contributions

MWL performed the experimental and method development duties as well as the organization of the article. PNN conceptualized the research project idea. Both KMD and PNN read and approved the final article.

Funding

The authors wish to thank Department of Science and Technology (DST, South Africa)/National Nanoscience Postgraduate Teaching and Training Programme (NNPTTP) and National Research Foundation (NRF, South Africa, grant no. 99270) for their financial support.

Availability of data and materials

Not applicable

Competing interests

The authors declare that they have no competing interests.

Author details

[1]Department of Chemical Sciences (Former Applied Chemistry), University of Johannesburg, Doornfontein Campus, P.O. Box 17011, Doornfontein 2028, South Africa. [2]DST/Mintek Nanotechnology Innovation Centre, University of Johannesburg, Doornfontein 2028, South Africa. [3]DST/NRF SARChI Chair: Nanotechnology for Water, University of Johannesburg, Doornfontein 2028, South Africa.

Received: 28 February 2019 Accepted: 20 June 2019
Published online: 02 July 2019

References

Andreozzi R, Marotta R, Pinto G, Pollio A. Carbamazepine in water: persistence in the environment, ozonation treatment and preliminary assessment on algal toxicity. Water Res. 2002;36:2869–77.

Asfaram A, Ghaedi M, Goudarzi A, Soylak M. Comparison between dispersive liquid–liquid microextraction and ultrasound-assisted nanoparticles-dispersive solid-phase microextraction combined with microvolume spectrophotometry method for the determination of Auramine-O in water samples. RSC Adv. 2015a;5:39084–96.

Asfaram A, Ghaedi M, Goudarzi A, Soylak M, Langroodi SM. Magnetic nanoparticle based dispersive micro-solid-phase extraction for the determination of malachite green in water samples: optimized experimental design. New J Chem. 2015b;39:9813–23.

Asgari S, Bagheri H, Es-Haghi A, AminiTabrizi R. An imprinted interpenetrating polymer network for microextraction in packed syringe of carbamazepine. J Chromatogr A. 2017;1491:1–8.

Aslani A, Arefi MR, Babapoor A, Amiri A, Beyki-Shuraki K. Solvothermal synthesis, characterization and optical properties of ZnO, ZnO–MgO and ZnO–NiO, mixed oxide nanoparticles. Appl Surf Sci. 2011;257:4885–9.

Asmaly HA, Abussaud B, Saleh TA, Gupta VK, Atieh MA. Ferric oxide nanoparticles decorated carbon nanotubes and carbon nanofibers: from synthesis to enhanced removal of phenol. J Saudi Chem Soc. 2015;19:511–20.

Bahmaei M, Khalilian F, Mashayekhi HA. Determination of carbamazepine in biological samples using ultrasound-assisted emulsification micro-extraction and gas chromatography. J Chem Health Risks. 2018;8(3):223–38.

Behbahani M, Najafi F, Bagheri S, Bojdi MK, Salarian M, Bagheri A. Application of surfactant assisted dispersive liquid–liquid microextraction as an efficient sample treatment technique for preconcentration and trace detection of zonisamide and carbamazepine in urine and plasma samples. J Chromatogr A. 2013;1308:25–31.

Chaba JM, Nomngongo PN. Preparation of V2O5-ZnO coated carbon nanofibers: application for removal of selected antibiotics in environmental matrices. J Water Process Eng. 2018;23:50–60.

Chen C-H, Lin S-K. Carbamazepine treatment of bipolar disorder: a retrospective evaluation of naturalistic long-term outcomes. BMC Psychiatry. 2012;12:47.

Clara M, Strenn B, Kreuzinger N. Carbamazepine as a possible anthropogenic marker in the aquatic environment: investigations on the behaviour of carbamazepine in wastewater treatment and during groundwater infiltration. Water Res. 2004;38:947–54.

Dhineshbabu NR, Karunakaran G, Suriyaprabha R, Manivasakan P, Rajendran V. Electrospun MgO/Nylon 6 hybrid nanofibers for protective clothing. Nano-Micro Lett. 2014;6:46–54.

Dinesh V, Biji P, Ashok A, Dhara S, Kamruddin M, Tyagi A, Raj B. Plasmon-mediated, highly enhanced photocatalytic degradation of industrial textile dyes using hybrid ZnO@ Ag core–shell nanorods. RSC Adv. 2014;4:58930–40.

dos Santos RC, Kakazu AK, Santos MG, Silva FAB, Figueiredo EC. Characterization and application of restricted access carbon nanotubes in online extraction of anticonvulsant drugs from plasma samples followed by liquid chromatography analysis. J Chromatogr B. 2017;1054:50–6.

Fortuna A, Sousa J, Alves G, Falcão A, Soares-da-Silva P. Development and validation of an HPLC-UV method for the simultaneous quantification of carbamazepine, oxcarbazepine, eslicarbazepine acetate and their main metabolites in human plasma. Anal Bioanal Chem. 2010;397:1605–15.

Gierbolini J, Giarratano M, Benbadis SR. Carbamazepine-related antiepileptic drugs for the treatment of epilepsy-a comparative review: Taylor & Francis. 2016; 17(7)885–888.

Gros M, Petrović M, Barceló D. Multi-residue analytical methods using LC-tandem MS for the determination of pharmaceuticals in environmental and wastewater samples: a review. Anal Bioanal Chem. 2006;386:941–52.

Halling-Sørensen B, Nielsen SN, Lanzky P, Ingerslev F, Lützhøft HH, Jørgensen S. Occurrence, fate and effects of pharmaceutical substances in the environment-a review. Chemosphere. 1998;36:357–93.

Heberer T. Occurrence, fate, and removal of pharmaceutical residues in the aquatic environment: a review of recent research data. Toxicol Lett. 2002a;131:5–17.

Heberer T. Tracking persistent pharmaceutical residues from municipal sewage to drinking water. J Hydrol. 2002b;266:175–89.

Hoff RB, Pizzolato TM, Peralba MCR, Díaz-Cruz MS, Barceló D. Determination of sulfonamide antibiotics and metabolites in liver, muscle and kidney samples by pressurized liquid extraction or ultrasound-assisted extraction followed by liquid chromatography–quadrupole linear ion trap-tandem mass spectrometry (HPLC–QqLIT-MS/MS). Talanta. 2015;134:768–78.

Kaerkitcha N, Chuangchote S, Sagawa T. Control of physical properties of carbon nanofibers obtained from coaxial electrospinning of PMMA and PAN with adjustable inner/outer nozzle-ends. Nanoscale Res Lett. 2016;11:186.

Karimi MA, Hatefi-Mehrjardi A, Kabir AA, Zaydabadi M. Synthesis, characterization, and application of MgO/ZnO nanocomposite supported on activated carbon for photocatalytic degradation of methylene blue. Res Chem Intermed. 2015; 41:6157–68.

Larsen TA, Lienert J, Joss A, Siegrist H. How to avoid pharmaceuticals in the aquatic environment. J Biotechnol. 2004;113:295–304.

Lübbert C, Baars C, Dayakar A, Lippmann N, Rodloff AC, Kinzig M, Sörgel F. Environmental pollution with antimicrobial agents from bulk drug manufacturing industries in Hyderabad, South India, is associated with dissemination of extended-spectrum beta-lactamase and carbapenemase-producing pathogens. Infection. 2017;45:479–91.

Metcalfe CD, Miao XS, Koenig BG, Struger J. Distribution of acidic and neutral drugs in surface waters near sewage treatment plants in the lower Great Lakes, Canada. Environ Toxicol Chem. 2003;22:2881–9.

Miao X-S, Yang J-J, Metcalfe CD. Carbamazepine and its metabolites in wastewater and in biosolids in a municipal wastewater treatment plant. Environ Sci Technol. 2005;39:7469–75.
Mirjana S, et al. Development and validation of SPE-HPLC method for the determination of carbamazepine and its metabolites carbamazepine epoxide and carbamazepine trans-diol in plasma. J Serb Chem Soc. 2012;77:1423–36.
Murdoch K. Pharmaceutical pollution in the environment: issues for Australia, New Zealand and Pacific island countries: National Toxic Network; 2015. p. 1–36. www.ntn.org.au
Nyaba L, Matong JM, Nomngongo PN. Nanoparticles consisting of magnetite and Al^2O^3 for ligandless ultrasound-assisted dispersive solid phase microextraction of Sb, Mo and V prior to their determination by ICP-OES. Microchim Acta. 2016;183:1289–97.
Öllers S, Singer HP, Fässler P, Müller SR. Simultaneous quantification of neutral and acidic pharmaceuticals and pesticides at the low-ng/l level in surface and waste water. J Chromatogr A. 2001;911:225–34.
Patrolecco L, Ademollo N, Grenni P, Tolomei A, Caracciolo AB, Capri S. Simultaneous determination of human pharmaceuticals in water samples by solid phase extraction and HPLC with UV-fluorescence detection. Microchem J. 2013;107:165–71.
Rezaee M, Mashayekhi HA. Solid-phase extraction combined with dispersive liquid–liquid microextraction as an efficient and simple method for the determination of carbamazepine in biological samples. Anal Methods. 2012;4: 2887–92.
Sacher F, Lange FT, Brauch H-J, Blankenhorn I. Pharmaceuticals in groundwaters: analytical methods and results of a monitoring program in Baden-Württemberg, Germany. J Chromatogr A. 2001;938:199–210.
Swart K, Sutherland F, Van Essen G, Hundt H, Hundt A. Determination of fluspirilene in human plasma by liquid chromatography–tandem mass spectrometry with electrospray ionisation. J Chromatogr A. 1998;828:219–27.
Ternes TA. Occurrence of drugs in German sewage treatment plants and rivers. Water Res. 1998;32:3245–60.
Vosough M, Ghafghazi S, Sabetkasaei M. Chemometrics enhanced HPLC–DAD performance for rapid quantification of carbamazepine and phenobarbital in human serum samples. Talanta. 2014;119:17–23.
Zhang Y, Xu S, Luo Y, Pan S, Ding H, Li G. Synthesis of mesoporous carbon capsules encapsulated with magnetite nanoparticles and their application in wastewater treatment. J Mater Chem. 2011;21:3664–71.

Publisher's Note